Radium Ion Spectroscopy

Giri, Gouri Shankar

Appendix A

Discussion of Ion Trapping

In this section the basic principles of trapping ions are discussed. Elaborate treatment of these principles and related techniques can be found in [121, 122].

Earnshaw's theorem states that: *A charge acted on by electrostatic forces can not rest in stable equilibrium in an electric field.* It implies that it is not possible to generate a minimum of the electrostatic potential in free space. Hence it is not possible to confine an ion using a purely electrostatic field. However it is possible to circumvent Earnshaw's theorem by superimposing a magnetic field to create a *Penning trap* or by superimposing a time varying electric field to create a *Paul trap*. We will discuss the Paul traps and the underlying physics [107, 123]. Discussion of Penning traps can be found in [124].

A.1 Paul Trap

The principle of confining ions in a Paul trap can be understood using a simple mechanical analogue, a ball moving on a saddle-shaped surface which is shown in Fig. A.1. Rotation of the saddle-shaped surface, at a suitable speed about a vertical axis, can prevent the ball rolling off the sides of the saddle and gives stable confinement. The gravitational potential energy of a ball on a saddle-shaped surface has the same form as the potential energy of an ion close to a saddle point of the electrostatic potential in a Paul trap.

Confinement of charged particles requires a potential minimum at some point in space in order that the corresponding force is directed toward that point in all three dimensions. In general, the dependence of the magnitude of this force on the coordinates can have any arbitrary form. However, it is convenient to have a binding force that is harmonic, since it can simplify the analytical description of

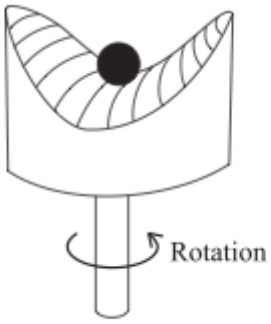

Fig. A.1: Mechanical model of dynamic stability. A rotating saddle shaped surface provides dynamic stability to a ball on this surface.

particle motion.

Particles are elastically bound to an axis or a coordinate system in space if a binding force acts on them which increases linearly with their distance r, for which we have

$$F \propto -r. \tag{A.1}$$

If $U = Q\Phi$ is the potential energy, then it follows from $F = -\nabla U$ that, the potential Φ is a quadratic function in cartesian coordinates

$$\Phi = \frac{\varphi}{2{r_0}^2}(\alpha x^2 + \beta y^2 + \gamma z^2). \tag{A.2}$$

The potential has to satisfy Laplace's equation in free space ($\nabla^2\Phi$=0). $\nabla^2\Phi$=0 imposes the condition $\alpha + \beta + \gamma$=0. There are two simple ways to satisfy this condition. $\alpha = 1 = -\beta$, γ=0 results in a two-dimensional field whereas $\alpha = \gamma = 1$, $\beta = -2$ results in a three-dimensional configuration,

$$\Phi = \frac{\varphi}{2{r_0}^2}(x^2 - y^2) \qquad \text{for } \alpha\text{=}1\text{=-}\beta,\ \gamma\text{=}0 \tag{A.3}$$

$$= \frac{\varphi}{2{r_0}^2}(x^2 + y^2 - 2z^2) \qquad \text{for } \alpha\text{=}\beta\text{=}1,\ \gamma\text{=-}2. \tag{A.4}$$

Trapping of Particles in a Two Dimensional Quadrupole Trap

A two dimensional configuration as in Eq. A.3 can be generated by four hyperbolically shaped electrodes linearly extended in the z-direction as shown in the Fig. A.2.

The filed strength is given by the field equations

$$E_x = -\frac{\varphi_0}{{r_0}^2}x, \quad E_y = \frac{\varphi_0}{{r_0}^2}y, \quad E_z = 0. \tag{A.5}$$

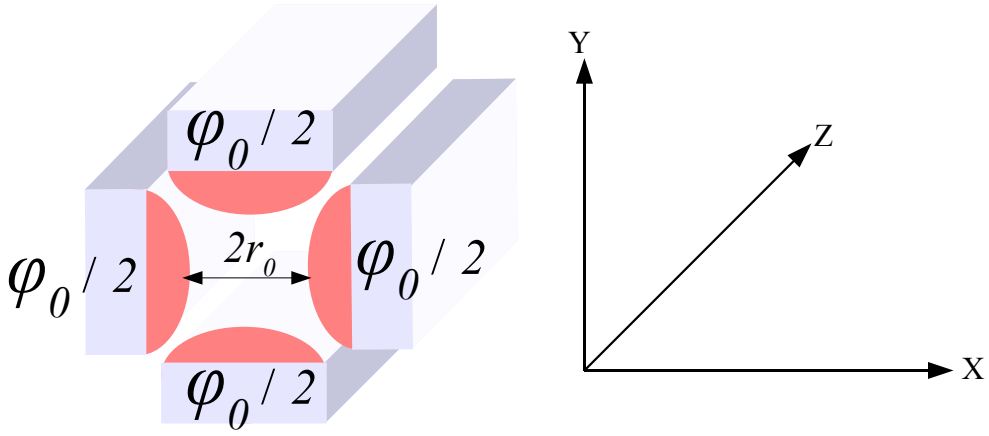

Fig. A.2: Electrode structure for a two dimensional quadrupole trap

If ions are injected along the z-direction, the electric field equations (A.5) suggest that the ions will perform harmonic oscillations in the x-z plane. However, the amplitude of oscillation in the y-direction will increase due to the opposite sign of the field E_y. This will create instability and as a result the ions will hit the electrodes and hence will be lost from the trap. Such a situation can easily be avoided by applying an additional voltage (φ_0) that is alternating in time. φ_0 can be made periodic with a DC voltage U and an RF voltage V with driving frequency ω

$$\varphi_0 = U + V\cos\omega t. \tag{A.6}$$

If the voltage φ_0 is applied between the electrode pairs then the potential on the electrodes is $\pm\varphi_0/2$. The non-relativistic motion of a charged particle in an electric filed is described by

$$\vec{F} = Q\vec{E}. \tag{A.7}$$

The equation of motion of the charged particle is written as

$$\ddot{r} = \frac{Q}{m}\vec{E}. \tag{A.8}$$

The equations of motion in x and y direction are given by

$$\ddot{x} = \frac{Q}{m}E_x = \frac{Q}{m}\left(-\frac{\varphi_0}{{r_0}^2}x\right), \qquad \ddot{y} = \frac{Q}{m}E_y = \frac{Q}{m}\left(\frac{\varphi_0}{{r_0}^2}y\right). \tag{A.9}$$

These equations may be rewritten in a more conventional way as

$$\frac{d^2x}{dt^2} + \frac{Q}{m{r_0}^2}\left(U + V\cos\omega t\right)x = 0 \tag{A.10}$$

$$\frac{d^2y}{dt^2} - \frac{Q}{m{r_0}^2}\left(U + V\cos\omega t\right)y = 0. \tag{A.11}$$

The differential equations A.10 and A.11 are knows as *Mathieu equations*. With some simple mathematical manipulation, the Mathieu equations can be written using dimensionless parameters a, q and τ. With τ=ωt/2 and $\frac{d^2}{dt^2} \equiv \frac{\omega^2}{2}\frac{d^2}{d\tau^2}$, the Mathieu equations can be written as

$$\frac{d^2x}{d\tau^2} + (a + 2q\cos 2\tau)x = 0 \tag{A.12}$$

$$\frac{d^2y}{d\tau^2} - (a + 2q\cos 2\tau)y = 0, \tag{A.13}$$

where the dimensionless parameters a, q and τ are given by

$$a = \frac{4QU}{m{r_0}^2\omega^2}, \quad q = \frac{2QV}{m{r_0}^2\omega^2}, \quad \tau = \frac{\omega t}{2}. \tag{A.14}$$

These dimensionless parameters are called Mathieu parameters. As expressed in Eq. A.14, the Mathieu parameters a and q depend on the DC voltage U and the RF voltage V respectively. Both parameters also depend on the charge-to-mass ratio Q/m of the ion and quadratically on the distance $2r_0$ between opposite rods and the oscillation frequency ω.

A.2 Stability of Ions in a Trap

The Mathieu equations have both stable and unstable solutions. In case of stable situation, the ions oscillate in the xy-plane with limited amplitude and they can travel through the quadrupole field along the z-direction without hitting the electrodes. In case of unstable solution, the amplitude of oscillation in the x, y, or both directions grows and the ions will be lost. The stability of the ions in the trap depends only on the Mathieu parameters a and q, and not on the initial parameters of the ion motion, Hence it is important to know the zones of stability in the a-q map, also know as *Mathieu stability diagram*.

The trapped ions are stable in all regions of Mathieu stability diagram where x-stable and y-stable portions overlap. As shown in Fig. A.3, there exist several regions of stability in the Mathieu stability diagram at high value of a and q. But the most used stability region is defined by $q < 0.91$ and small a. For fixed values of r_0, ω, U, and V, all ions with the same charge-to-mass ratio Q/m have the same operating point in the Mathieu stability diagram. Since a/q is equal to $2U/V$ and is independent of the mass m, all masses lie along the operating line a/q=constant (Fig. A.4).

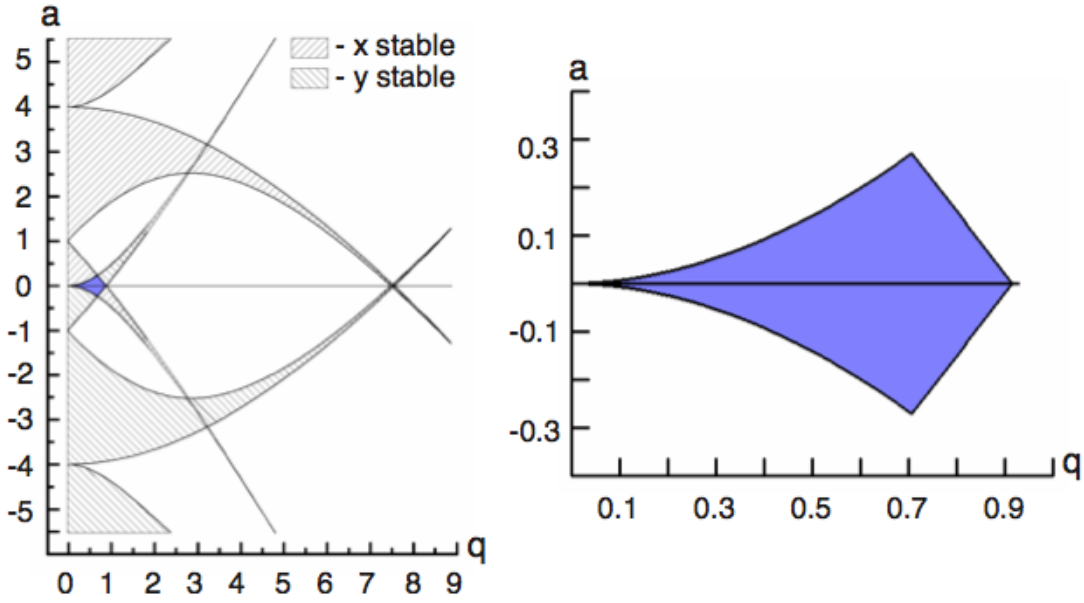

Fig. A.3: Mathieu stability diagrams in a two dimensional quadrupole trap. The right figure indicates the zone of stability. Adapted from [19].

Radial confinement of ions in a linear Paul trap relies on the inhomogeneity of electric fields between the electrodes. Only in a homogenous field the time-dependent term of the force cancels out in the time average. But in a quadrupole field, which is a periodic inhomogeneous field, there is a small average force left pointing toward the center of the trap which enables the ions to traverse the quadrupole field without hitting the electrodes. Hence the motion of the ions around the z axis can be stable with limited amplitude in x and y directions. In a quadrupole field the potential at the geometrical center between the electrodes is zero and it increases with the distance from center according to Eq. A.3. This field inhomogeneity leads to a small average force in the direction towards the low field regions (closer to the center of trap), resulting in a *pseudo potential well* for the ions [125]. With r as the distance from the trap axis the pseudo potential $\Phi_{PS}(r)$ for the ions confined by the RF field ($V\cos\omega t$) is given by

$$\Phi_{PS}(r) = \frac{qV}{4r_0^2}r^2. \tag{A.15}$$

A.3 Macromotion and Micromotion

The stable motion of ions in the RF quadrupole field can be decomposed into two separate oscillatory motions, the micromotion and the macromotion. The

micromotion is caused directly by the electric field oscillations. Thus, it has the same frequency ω as that of RF, except it is out of phase with the field by π. It also follows the strength of the electric field. The macromotion or secular motion is associated with the pseudo potential and it has a lower frequency (ω_{macro}) which is related to the RF frequency (ω) as

$$\omega_{macro} = \frac{q}{2\sqrt{2}}\omega. \tag{A.16}$$

Trapping of Particles in a Three Dimensional Quadrupole Trap

Trapping of particles in a three dimensional quadrupole field is very similar to the two dimensional case as discussed before. A three dimensional configuration as in Eq. A.4. can be generated in many different ways, e.g., with a hyperbolically shaped ring electrode and two hyperbolic rotationally symmetric caps. The field equations in the three dimensional case are given by

$$E_x = \frac{\varphi_0}{{r_0}^2}x, \quad E_y = \frac{\varphi_0}{{r_0}^2}y, \quad E_z = -2\frac{\varphi_0}{{r_0}^2}z. \tag{A.17}$$

Using similar mathematical treatment as shown in the two dimensional case, one can arrive at the conclusion that the equations of motions of the ions in a three dimensional quadrupole trap can be represented by similar Mathieu equations

$$\frac{d^2x}{d\tau^2} - (a + 2q\cos 2\tau)x = 0 \tag{A.18}$$

$$\frac{d^2y}{d\tau^2} - (a + 2q\cos 2\tau)y = 0 \tag{A.19}$$

$$\frac{d^2z}{d\tau^2} + (a + 2q\cos 2\tau)z = 0, \tag{A.20}$$

where the dimensionless parameters a, q and τ are given by

$$a_x = a_y = 2a_z = \frac{4QU}{m{r_0}^2\omega^2} \tag{A.21}$$

$$q_x = q_y = 2q_z = \frac{2QV}{m{r_0}^2\omega^2} \tag{A.22}$$

$$\tau = \frac{\omega t}{2}. \tag{A.23}$$

Accordingly the region of stability in the a-q map for a three dimensional trap has a different shape, as shown in Fig. A.4. Similar to the two dimensional counterpart, the motion of ions in a three dimensional quadrupole trap is described as a slow secular motion modulated with a micromotion. The pseudo potential [125]

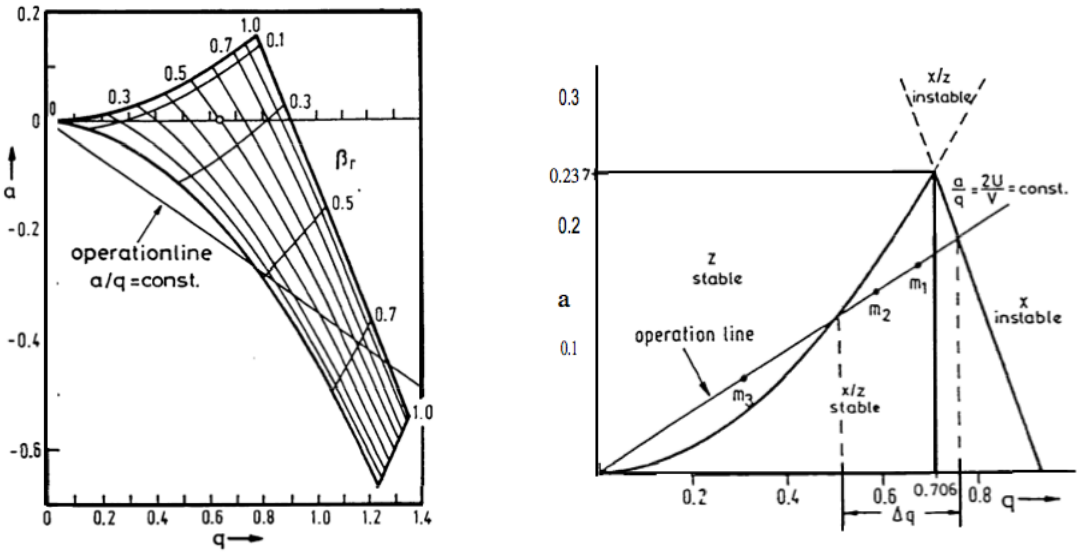

Fig. A.4: Mathieu stability diagram in a quadrupole trap for two dimensional (right) and three dimensional (left) case . Adapted from [123].

in a three dimensional quadrupole field is given by

$$\Phi_{PS} = D\frac{x^2 + y^2 + 4z^2}{r_0^2 + 2z_0^2}, \tag{A.24}$$

where, D is the potential depth. Both in two and three dimensional quadrupole traps the radio frequency voltage amounts to be a few hundred volts and potential depth is of the order of 10 volts. The width of the potential well is defined by the geometrical dimension of the trap.

Appendix B

Discussion of Hyperfine Structure

B.1 Hyperfine Structure Interval

The term hyperfine structure refers to a structure in atomic spectra which results from the existence of spins and electromagnetic multipole moments of atomic nuclei. The interactions of these nuclear moments with the electrons lead to an additional splitting of the spectral lines which is knows as the hyperfine structure.

B.2 Spins and Electromagnetic Multipole Moments

If the nucleus has a nonzero nuclear spin I, then it is said to possess a nuclear angular momentum $\vec{I}$, where

$$|\vec{I}| = \sqrt{I(I+1)}\hbar. \tag{B.1}$$

The quantum number I may be integral or half integral[1]. Similar to electronic angular momentum, the nuclear angular momentum is observable along the quantization axis, e.g., in the z-direction where an applied magnetic field is oriented. The x and y components have time averages equal to zero and hence are not observable. For the z-component $(\vec{I})_z$=$m_I\hbar$ with m_I=*I, I-1, ..., 0, ..., -I+1, I.* Thus there are $2I+1$ possible orientations of nuclear angular moment relative to

[1]Stable atomic nuclei are known with $0 < I < 15/2$.

the quantization axis, corresponding to the possible values of nuclear magnetic quantum number m_I.

B.3 The Hyperfine Interaction

In addition to spin a nucleus has also electromagnetic multipole moments. The interactions between those moments and the electromagnetic field produced by the electrons at the nucleus are responsible for the hyperfine structure.

By arguments of parity and time-reversal symmetry the only non-vanishing multipole (2^k-pole) moments, apart from the electric charge for k=0, are the magnetic moments for odd k and the electric moments for even k. Interactions of the higher order multipole moments ($k\geq3$) with the electrons are negligibly small. Hence the two lowest orders of interaction, i.e., the magnetic dipole interaction and the electric quadrupole interaction are of physical importance with regard to hyperfine structure.

B.3.1 Magnetic Dipole Interaction

Magnetic dipole interaction is the interaction of a point nuclear magnetic moment $\vec{\mu}_I$ with the magnetic field $\vec{B}_J$ produced by the electrons at the nucleus. The nuclear magnetic moment $\vec{\mu}_I$ is connected with nuclear angular momentum $\vec{I}$ as

$$\vec{\mu}_I = \gamma\vec{I} = \frac{g_I\mu_N}{\hbar}\vec{I}, \tag{B.2}$$

where γ is the *gyromagnetic ratio*. g_I is the nuclear g-factor. $\mu_N = e\hbar/2m_p$ is the unit of nuclear magnetic moment (nuclear magneton) which is analogous to the Bohr magneton $\mu_B = e\hbar/2m_e$.
Following the quantization rules for the angular momentum

$$(\vec{\mu}_I)_z = \frac{g_I\mu_N}{\hbar}(\vec{I})_z = g_I\mu_N m_I. \tag{B.3}$$

The Hamiltonian for the magnetic dipole interaction is given by

$$H_D = -\vec{\mu}_I \cdot \vec{B}_J. \tag{B.4}$$

This is to be treated as a small perturbation. $\vec{\mu}_I$ depends on nuclear coordinates only and $\vec{B}_J$ depends on electronic coordinates only. With an adoption of IJ coupling approximation, one can write $\vec{B}_J \propto \vec{J}$, as $\vec{B}_J$ operates in the space of electronic coordinates only. Hence Eq. B.4 can take the form

$$H_D = A\vec{I} \cdot \vec{J}, \tag{B.5}$$

where A is the *hyperfine structure constant*, an experimentally measurable quantity. According to IJ coupling approximation

$$\vec{F} = \vec{I} + \vec{J} \tag{B.6}$$

$$\vec{F}^2 = (\vec{I} + \vec{J})^2 = \vec{I}^2 + \vec{J}^2 + 2\vec{I}.\vec{J} \tag{B.7}$$

$$\vec{I}.\vec{J} = \frac{1}{2}\left[\vec{F}^2 - \vec{I}^2 - \vec{J}^2\right]. \tag{B.8}$$

To first order[2], the energy shift of a level J is given by the expectation value of the interaction Hamiltonian (for magnetic dipole interaction) of Eq. B.5

$$\Delta E_D = \langle IJFm_F|H_D|IJFm_F\rangle \tag{B.9}$$

$$= \langle IJFm_F|A\vec{I}\cdot\vec{J}|IJFm_F\rangle \tag{B.10}$$

$$= \frac{A}{2}\left[F(F+1) - J(J+1) - I(I+1)\right]. \tag{B.11}$$

In summary, a level with well-defined total angular momentum J splits into hyperfine states, labelled by F, which are $(2F+1)$-fold degenerate. The hyperfine structure constant A is a measure of the splitting and there is an interval rule,

$$\Delta E_F - \Delta E_{F-1} = AF. \tag{B.12}$$

F has $2I+1$ values for $I<J$ or $2J+1$ values for $J\leq I$. The electric dipole selection rule for F is $\Delta F=0,\pm1$ while $F=0 \rightarrow F=0$ is forbidden.

B.3.2 Electric Quadrupole Interaction

Electric quadrupole interaction is the interaction between the nuclear electric quadrupole moment and the electric field of electrons. The nuclear electric quadrupole moment depends on the nuclear charge distribution. For nucleus with $I > 1/2$, the quadrupole moment is non-zero. It is positive for prolate[3] and negative for oblate[4] charge distribution.

The quadrupole interaction causes a shift of the hyperfine levels. In first order, the energy shift is

$$\Delta E_Q = \langle IJFm_F|H_Q|IJFm_F\rangle \tag{B.13}$$

$$= \frac{B}{4}\left[\frac{\frac{3}{2}K(K+1) - 2I(I+1)J(J+1)}{I(2I-1)J(2J-1)}\right], \tag{B.14}$$

[2]Consideration of configuration mixing and relativistic effects, though important in hyperfine structure, is beyond the scope of this thesis.

[3]Cigar-shaped charge distribution, elongated along the direction of I.

[4]Pin-cushioned shaped charge distribution, flattened perpendicular to I.

where $K = [F(F+1) - J(J+1) - I(I+1)]$. B is another hyperfine structure constant. The quadrupole interaction vanishes for S terms because of spherically symmetric electron charge distribution. The quadrupole interaction also vanishes unless $I \geq 1$, $J \geq 1$.

Combining the magnetic dipole and electric quadrupole shifts from Eq. B.11 and Eq. B.14, the hyperfine structure interval can be written as

$$\Delta E_{HFS} = \frac{A}{2}K + \frac{B}{4}\left[\frac{\frac{3}{2}K(K+1) - 2I(I+1)J(J+1)}{I(2I-1)J(2J-1)}\right]. \tag{B.15}$$

This shows that the electric quadrupole interaction gives rise to a departure from the interval rule, because its dependence on F is different from that of magnetic dipole interaction. When B/A is sufficiently large the order of F-levels may even be different from that when B/A=0.

Appendix C

Discussion of Isotope Shift

C.1 Isotope Shift

Bohr's model predicts that for a transition between energy levels with principal quantum numbers n_1 and n_2, an atom emits light with a wave number given by

$$\tilde{\nu}_\infty = R_\infty \left(\frac{1}{n_1^2} - \frac{1}{n_2^2} \right), \tag{C.1}$$

where R_∞ is the Rydberg constant. The subscript ∞ indicates that the nucleus is assumed to be infinitely massive.
But the spectral lines in hydrogen obey the mathematical formula

$$\tilde{\nu} = R_H \left(\frac{1}{n_1^2} - \frac{1}{n_2^2} \right). \tag{C.2}$$

There is a subtle difference between R_∞ and R_H. In reality, the electron and the nucleus move around the center of mass of the system. Mathematically R_∞ can be expressed as

$$hcR_\infty = \frac{(e^2/4\pi\varepsilon_0)^2 m_e}{2\hbar^2}. \tag{C.3}$$

For a hydrogen nucleus of finite mass m_p,

$$hcR_H = \frac{(e^2/4\pi\varepsilon_0)^2 m}{2\hbar^2}, \tag{C.4}$$

where m is the reduced mass of the electron, $\frac{m_e m_p}{m_e + m_p}$.
Now it is evident that

$$R_H = R_\infty \frac{m_p}{m_e + m_p}. \tag{C.5}$$

This reduced mass correction is not the same for different isotopes of a particular element, e.g., hydrogen and deuterium. This leads to a measurable difference in

the frequency of a spectral line for two different isotopes. This is called *isotope shift*. For many-electron atoms the nuclear properties that contribute towards isotope shifts are the finite mass (*mass effect*) and the extended charge distribution of the nucleus (*field effect*).

C.2 Mass Effect

The mass effect may be treated by considering the kinetic energy operator in Schrödinger's equation

$$T = \frac{\vec{P}_N^2}{2M_N} + \sum_i \frac{\vec{p}_i^2}{2m_e}, \tag{C.6}$$

where P_N and M_N are the momentum and mass of the nucleus, while p_i and m_e are the momentum and mass of the i^{th} electron. By following the principle of conservation of momentum for a stationary atom,

$$\vec{P}_N = -\sum_i \vec{p}_i. \tag{C.7}$$

Hence,

$$T = \frac{(\sum_i p_i)^2}{2M_N} + \frac{\sum_i p_i^2}{2m_e} \tag{C.8}$$

$$= \frac{\sum_i p_i^2}{2M_N} + \frac{1}{M_N}\sum_{i>j} p_i \cdot p_j + \frac{\sum_i p_i^2}{2m_e}. \tag{C.9}$$

The second term in Eq. C.9, which contains the dot product of electron momenta, can be ignored for single electron systems, e.g., hydrogen and deuterium. The remaining two terms can be combined with the introduction of the reduced mass $m = \frac{m_e m_p}{m_e + m_p}$. Thus an energy level $E(M_N)$ for an atom whose nucleus has a finite mass M_N is raised above the fictitious level (E_∞) for a 'theoretical' atom whose nucleus is infinitely heavy. This can be expressed as

$$E(M_N) = E_\infty \frac{M_N}{m_e + M_N}. \tag{C.10}$$

In terms of wavenumber

$$\tilde{\nu} = \tilde{\nu}_\infty \frac{M_N}{m_e + M_N} \tag{C.11}$$

$$\simeq \tilde{\nu}_\infty \left(1 - \frac{m_e}{M_N}\right). \tag{C.12}$$

However, $\tilde{\nu}_\infty$ can not be measured and only the difference in wave numbers between two isotopes of an element can be observed. Considering two isotopes with nuclear masses $M_N^{'}$ and $M_N^{''}$, the wavenumber shift for the observed spectral line is

$$\Delta\tilde{\nu}_{mass} = \nu_{M_N^{''}} - \nu_{M_N^{'}} \tag{C.13}$$

$$\simeq \tilde{\nu}_\infty \left[\left(1 - \frac{m_e}{M_N^{''}}\right) - \left(1 - \frac{m_e}{M_N^{'}}\right)\right] \tag{C.14}$$

$$\simeq \tilde{\nu}_\infty m_e \left(\frac{M_N^{''} - M_N^{'}}{M_N^{''} M_N^{'}}\right) \tag{C.15}$$

$$\simeq \frac{m_e \delta M_N}{M_N^{'} - M_N^{''}} \tilde{\nu}_\infty, \tag{C.16}$$

where the isotope of greater mass has the larger wavenumber. This phenomenon is known as *normal mass shift*. This shift is the largest for hydrogen-deuterium. Since the mass shift is proportional to $\frac{1}{M^2}$, the mass effect is small for heavy elements.

For multi-electron systems, the cross term in Eq. C.9 can not be neglected and it leads to an additional isotope shift known as the *specific mass shift*. Since the cross term involves a correlation between the motions of electron pairs, this effect is very difficult to calculate for many electron atoms. For lighter elements the specific mass shift has the same order of magnitude as the normal mass shift. But in heavy elements, the effect is small.

C.3 Field Effect

Isotope shifts originating from the variations of the nuclear charge distribution from one isotope to another is referred to as field shifts. Such shifts are of physical significance because the measurement of field shifts in spectral lines helps one study the size and shape of nucleus as a function of neutron number. The field effects can be treated by understanding the electric monopole interaction between the nucleus and the electrons, and considering its departure (for real nuclei) from the pure coulomb potential of a point nuclear charge. To probe the nuclear charge distribution the s-electron must be considered whose charge density does not vanish in the region of the nucleus[1]. Then an isotope shift is expected in a spectral line for which the number of s-electrons is different in the

[1]Relativistically, $P_{1/2}$ electrons also have a non-vanishing charge density in the region of nucleus. Other electrons with $l \neq 0$ have a negligible charge density.

two terms involved in the transition. Without considering relativistic and higher order perturbation treatment it is possible to estimate an order of magnitude of the field effects in heavy elements.

For simplicity we consider a nuclear model which assumes a spherically symmetric nuclear charge distribution. For example, the liquid drop model assumes a spherically symmetric nuclear charge distribution with radius r_0 given by

$$r_0 \simeq 1.2 \times A^{1/3} \text{ fm}. \tag{C.17}$$

We consider the isotope shift of a term for two isotopes whose nuclear radii differ by

$$\frac{\delta r_0}{r_0} = \frac{1}{3}\frac{\delta A}{A}. \tag{C.18}$$

This field effect, in particular, is known as *volume shift*. In first order, the contribution to the energy shift of a term for each electron is the expectation value of the electrostatic potential energy difference $V(r) - V(r_0)$, where $V(r)$ and $V_0(r)$ are the potential energies appropriate to an extended nucleus and to a point nucleus respectively. Thus,

$$\Delta E_{volume} = \int_0^\infty \psi^* \left[V(r) - V_0(r)\right] \psi 4\pi r^2 \mathrm{d}r \tag{C.19}$$

$$\simeq |\psi(0)|^2 \int_0^{r_0} \left[V(r) - V_0(r)\right] 4\pi r^2 \mathrm{d}r. \tag{C.20}$$

The range of integration is restricted to $0 \leq r \leq r_0$ since, by Gauss's theorem, $V(r) = V_0(r)$ for $r \geq r_0$ and over this range the electron charge density (ρ_e) is assumed to be approximately constant

$$\rho_e \simeq -e|\psi(0)|^2. \tag{C.21}$$

For a point nuclear charge

$$V_0(r) = -\frac{Ze^2}{4\pi\varepsilon_0 r} \qquad (\text{ r} > 0\ ), \tag{C.22}$$

and, for a uniform nuclear charge distribution

$$V(r) = \frac{Ze^2}{4\pi\varepsilon_0 r_0}\left(-\frac{3}{2} + \frac{1}{2}\frac{r^2}{r_0^2}\right) \qquad (0 \leq \text{r} \leq \text{r}_0\ ). \tag{C.23}$$

By substitution in Eq. C.20 and upon integration

$$\Delta E_{volume} = \frac{4\pi}{10}|\psi(0)|^2 \frac{Ze^2}{4\pi\varepsilon_0} r_0^2. \tag{C.24}$$

The quantity that is directly related to the observation of isotope shift is the difference in ΔE_{volume} for the two isotopes

$$\delta(\Delta E_{volume}) = \frac{4\pi}{10}|\psi(0)|^2 \frac{Ze^2}{4\pi\varepsilon_0} 2r_0\delta r \tag{C.25}$$

$$= |\psi(0)|^2 \frac{Ze^2}{5\varepsilon_0} r_0^2 \frac{\delta r}{r_0} \tag{C.26}$$

$$= |\psi(0)|^2 \frac{Ze^2}{15\varepsilon_0} r_0^2 \frac{\delta A}{A} \qquad \text{using Eq. C.18.} \tag{C.27}$$

Hence the isotope shift caused by the volume effect is

$$\delta\tilde{\nu}_{volume} = \frac{\delta(\Delta E_{volume})}{hc} = |\psi(0)|^2 \frac{Ze^2}{15hc\varepsilon_0} r_0^2 \frac{\delta A}{A}. \tag{C.28}$$

Accurate determination of isotope shift through precision laser spectroscopy is an excellent way to probe nuclear shape and size, though it is necessary to know the absolute value of nuclear charge radius by another means.

Appendix D

Settings of the LEBL

Here the typical settings of various experimental parameters are recorded.

Table D.1: Settings of the low energy beam line and the linear Paul trap.

LEBL Component	HV Module	Channel A	Channel B
Lens A2	NIM08	0	1852
Wien Filter	NIM09	2890	2715
Bending Plate (Top/Bottom)	NIM10	2793	2818
Bending Plate (Left/Right)	NIM11	2808	180
Mirror	NIM24	1800	-
Einzel Lens 2 / Einzel Lens 1	NIM25	1650	1450

LEBL Component	HV Module	Channel Number							
		0	1	2	3	4	5	6	7
Bending Plate IN[a]	EHQ19	0	0	0	0	0	0	0	0
Bending Plate OUT[b]	EHQ20	115	85	32.5	25	0	0	0	0
Ion Trap DC Voltages	EHQ22	5	20	5	5	20	5	5	0

[a]Before Switch Point
[b]After Switch Point

LEBL Component	Setting
Drift Tube (After TI)	22 kHz, HV High: 84.0/30 kV, HV Low: 0 V
Drift Tube (Before Trap)	22 kHz, HV High : 80.6/30 kV, HV Low: -0.1 kV
Paul Trap	Frequency: 974.19 kHz, Voltage: 600 V (Peak-Peak)
Extraction TI	-6.85 kV
Deceleration Lens	-2.8 kV